Molecules and Cells

c-Cbl Acts as an E3 Ligase Against DDA3 for Spindle Dynamics and Centriole Duplication during Mitosis

Dasom Gwon[1,2], Jihee Hong[1,2], and Chang-Young Jang[1,*]

[1]Drug Information Research Institute, College of Pharmacy, Sookmyung Women's University, Seoul 04310, Korea, [2]These authors contributed equally to this work.
*Correspondence: cyjang@sookmyung.ac.kr
https://doi.org/10.14348/molcells.2019.0142
www.molcells.org

The spatiotemporal mitotic processes are controlled qualitatively by phosphorylation and qualitatively by ubiquitination. Although the SKP1-CUL1-F-box protein (SCF) complex and the anaphase-promoting complex/cyclosome (APC/C) mainly mediate ubiquitin-dependent proteolysis of mitotic regulators, the E3 ligase for a large portion of mitotic proteins has yet to be identified. Here, we report c-Cbl as an E3 ligase that degrades DDA3, a protein involved in spindle dynamics. Depletion of c-Cbl led to increased DDA3 protein levels, resulting in increased recruitment of Kif2a to the mitotic spindle, a concomitant reduction in spindle formation, and chromosome alignment defects. Furthermore, c-Cbl depletion induced centrosome over-duplication and centriole amplification. Therefore, we concluded that c-Cbl controls spindle dynamics and centriole duplication through its E3 ligase activity against DDA3.

Keywords: c-Cbl, centriole, centrosome, DDA3, E3 ligase, spindle dynamics

INTRODUCTION

Cell cycle progression in cell division is driven by the activity of cyclin-dependent kinases (CDKs) which are activated by phase-specific cyclins and inactivated by specific CDK inhibitors (CKIs) (Dulic et al., 1992). During cell cycle progression, CKIs like p21 and p27 act as negative CDK regulators in response to cell cycle checkpoint signals or DNA damage. Cyclin and CKI levels are modulated by transcriptional regulation and ubiquitin-mediated proteolysis (Nakayama and Nakayama, 2006). The SKP1-CUL1-F-box protein (SCF) complex and anaphase-promoting complex/cyclosome (APC/C) play key roles as E3 ligases in the proteolysis of cell cycle regulatory proteins including cyclins and CKIs (Skaar and Pagano, 2009). Both SCF and APC/C are RF-type E3s, which are composed of RF protein, scaffold protein, and adaptor proteins. The SCF complex employs F-box proteins, such as S-phase kinase associated protein 2, F-box and WD repeat domain containing 7, and β-transducin repeat containing protein, as receptor proteins for target protein-specific recognition in cell cycle control (Jin et al., 2004). Cell division cycle 20 and CDH1 confer substrate specificity to the APC/C in a manner similar to that of the F-box proteins in the SCF complex (Castro et al., 2005).

c-Cbl is a homolog of the v-Cbl oncogene and is known to code for an RF E3 ligase that targets receptor tyrosine kinases (RTKs), as well as a positive adaptor protein for RTK signaling (Schmidt and Dikic, 2005; Shrestha et al., 2018). The functional specificity of c-Cbl is determined by protein interaction motifs surrounding the RF, such as the N-terminal TK binding (TKB) domain and a proline-rich domain. Because the TKB

Received 28 June, 2019; revised 25 September, 2019; accepted 30 September, 2019; published online 14 November, 2019

eISSN: 0219-1032

contains a 4-helix bundle, a calcium binding EF hand, and an SH2 domain, c-Cbl can interacts with phosphorylated tyrosine residues on other proteins. The proline-rich domain also mediates interactions between c-Cbl and SH3-containing proteins in RTK signaling pathway. During epidermal growth factor receptor (EGFR) activation, growth factor receptor bound protein 2 (Grb2), the SH2 domain of which binds to autophosphorylated EGFR, recruits c-Cbl through an interaction between the proline-rich domain of c-Cbl and the SH3 domain of EGFR; c-Cbl competes with the guanine nucleotide exchange factor son-of-sevenless for binding to EGFR, thus negatively regulating Ras/mitogen-activated protein kinase (MAPK) (Jiang et al., 2003; Meisner et al., 1995). For adaptation to EGFR signaling, c-Cbl binds to autophosphorylated Tyr1045 through its SH2 domain, mediating EGFR ubiquitination and the subsequent desensitization of the proliferating signal by internalization of the active EGFR complex into endosome (Grovdal et al., 2004). In contrast, when phosphorylated on Tyr731, c-Cbl functions as a positive adaptor protein by recruiting phosphoinositide 3 kinase (PI3K) through interaction with the SH2 domain of PI3K, thus activating PI3K and downstream signaling pathways (Hunter et al., 1999).

DDA3 controls chromosome congression at metaphase and sister chromatid separation at anaphase by regulating spindle dynamics through the recruitment of the minus-end microtubule (MT) depolymerase, kinesin family member 2A (Kif2a) (Jang et al., 2008). The DDA3 complex contains MAP7 domain-containing protein 3 (Mdp3), which is a negative regulator against Kif2a recruitment and modulates minus-end spindle dynamics (Kwon et al., 2016). Because the level of DDA3 increases on mitotic entry and decreases on mitotic exit (Jang et al., 2008; Kwon et al., 2016), ASP7 has been suggested as the corresponding E3 ligase (Uematsu et al., 2016). Strikingly, we detected the presence of c-Cbl in the mitotic DDA3 complex through proteomic analysis. Furthermore, we demonstrated the mitotic functions of Cbl as an E3 ligase that ubiquitinates DDA3. Depletion of c-Cbl resulted in increased DDA3 levels, leading to several defects in mitotic processes including chromosome alignment, spindle formation, and centriole duplication. We concluded that c-Cbl regulates spindle dynamics and centriole duplication by acting as an E3 ligase that targets DDA3.

MATERIALS AND METHODS

Chemicals and antibodies

A rabbit antibody against DDA3 was raised against full-length recombinant DDA3 and affinity-purified as previously described (Jang et al., 2008; Wong and Fang, 2006). For Western blotting, the following antibodies were obtained from commercial sources (dilution, catalog number, and manufacturer): anti-Cyclin B1 (1:1,000, sc-245; Santa Cruz Biotechnology, USA), anti-HA (1:1,000, sc-7392; Santa Cruz Biotechnology), anti-Sas6 (1:500, sc-81431; Santa Cruz Biotechnology), anti-PLK4 (1:500, MABC544; Merck Millipore, USA), anti-c-Cbl (1:1,000, PA5-17453; Thermo Fisher Scientific, USA), anti-STIL (1:100, ab89314; Abcam, UK), anti-p38MAPK (1:10,000, GTX110720; GeneTex, USA), anti-HA (1:1,000, GTX29110; GeneTex), anti-Kif2a (1:1,000, NB500-180; Novus Biologicals, USA), horseradish peroxidase (HRP)-conjugated anti-mouse immunoglobulin G (IgG) F(ab') secondary antibody (1:2,000, ADI-SAB-100; Enzo Life Sciences, USA), and HRP-conjugated anti-rabbit IgG secondary antibody (1:2,000, 7074S; Cell Signaling Technology, USA). For immunostaining, the following antibodies were used (dilution, catalog number, and manufacturer): anti-HA (1:100, sc-7392; Santa Cruz Biotechnology), anti-Sas6 (1:50, sc-81431; Santa Cruz Biotechnology), anti-β-tubulin (1:200, Q-E7-S; Developmental Studies Hybridoma Bank, USA), anti-γ-tubulin (1:100, T6557; Sigma-Aldrich, USA), anti-centrin-1 (1:100, 12794-1-AP; Proteintech, USA), anti-c-NAP1 (1:100, 14498-1-AP; Proteintech), anti-PLK4 (1:100, MABC544; Merck Millipore), anti-Cbl (1:100, PA5-17453; Thermo Fisher Scientific), anti-pericentrin (1:100, ab4448; Abcam), anti-STIL (1:50, ab89314; Abcam), anti-Hec1 (1:200, GTX70268; GeneTex), anti-HA (1:100, GTX29110; GeneTex), anti-Kif2a (1:100, NB500-180; Novus Biologicals), Alexa Fluor 488 anti-rabbit secondary antibody (1:200, A11013; Invitrogen/Thermo Fisher Scientific, USA), and Alexa Fluor 594 anti-mouse secondary antibody (1:200, A32723; Invitrogen/Thermo Fisher Scientific).

The following chemicals were obtained from commercial sources: dimethyl sulfoxide (DMSO), and 4′,6-diamidine-2′-phenylindole dihydrochloride (DAPI) (Sigma-Aldrich); Tris base, NaCl, HCl, and sodium dodecyl sulfate (SDS) (Amresco, USA); paraformaldehyde (Electron Microscopy Sciences, USA); bovine serum albumin (BSA) (BioShop, Canada); Triton X-100, Mowiol, and N-propyl gallate (Thermo Fisher Scientific); Bradford protein assay kit (Thermo Fisher Scientific); polyvinylidene difluoride (PVDF) membranes and methanol (MilliporeSigma, USA); and protein molecular weight standard for electrophoresis (Bio-Rad Laboratories, USA).

Cell culture and transfection

HeLa cells were cultured in Dulbecco's modified Eagle's medium (DMEM; Welgene, Korea) supplemented with 10% fetal bovine serum (FBS; Invitrogen, USA), penicillin (100 U/ml), and 100 μg/ml streptomycin (Invitrogen). The cells were incubated at 37°C with 5% CO_2. siRNAs were synthesized by Genolution (Korea). The sequences targeting c-Cbl (siCbl-1 and siCbl-2) were 5'-GACACAUUUCGGAUUACUAUU-3' and 5'-GGAAGAUGGCAGUGAAUAUUU-3' and target to untranslatoinal region. The sequence targeting Seperase (siSeperase) was 5'-GCUUGUGAUGCCAUCCUGAUU-3'. The control siRNA (siGL2) was 5'-CGTACGCGGAATACTTCGATT-3'. siRNAs were transfected into HeLa cells using DharmaFect 1 (Dharmacon, USA) according to the manufacturer's instructions.

pCMV-HA-Cbl and pCMV-HA-ubiquitin plasmids were provided by S.H. Baek (Yeungnam University, Korea) (Choi et al., 2015; Huang et al., 2018). Lipofectamine 2000 (Invitrogen) was used for DNA transfection following the manufacturer's instructions. In brief, 250 ng DNA and Lipofectamine were diluted in Opti-MEM and incubated for 5 min at room temperature. The diluted DNA was combined with diluted Lipofectamine and incubated for 20 min at room temperature. Twenty-eight hours after incubation of DNA-Lipofectamine

complexes with the cells at 37°C in a CO_2 incubator, the cells were harvested for Western blotting or immunoprecipitation.

Immunofluorescent staining

HeLa cells were grown on a glass coverslip and fixed with methanol at –20°C for 30 min. Alternatively, cells on a coverslip were pre-extracted with BRB80-T buffer (80 mM PIPES, pH 6.8, 1 mM $MgCl_2$, 5 mM EGTA, and 0.5% Triton X-100) for 30 s and fixed with 4% paraformaldehyde for 15 min at room temperature. The fixed cells were then blocked with PBS-BT (1× phosphate-buffered saline [PBS], 3% BSA, and 0.1% Triton X-100) for 30 min at room temperature and incubated with primary antibodies diluted in PBS-BT for 30 min at room temperature, followed by incubation with secondary antibodies for 30 min at room temperature. To stain DNA, DAPI was added to PBS-BT at 1 μg/ml for 1 min. Z-image stacks were captured in 0.2 μm for kinetochore and 0.4 μm for other proteins on a Zeiss Axiovert 200M microscope controlled by AxioVision 4.8.2 (Carl Zeiss, Germany) using a 1.4 NA Plan-Apo ×100 oil immersion lens and an HRm CCD camera. Deconvolution was performed for all images using AutoDeblur v9.1 and AutoVisualizer v9.1 (AutoQuant Imaging, USA). Image stacks were represented as maximum intensity projections.

Live cell image

HeLa cells stably expressing GFP-Histone H2B were grown in glass chambers. Thirty minute before imaging, the medium was changed to pre-warmed Leibovitz's L-15 medium (Invitrogen) supplemented with 10% FBS (Invitrogen) and 2 mM L-glutamine (Invitrogen). Recoding was performed in a sealed growth chamber heated to 37°C on a Zeiss Axiovert 200M microscope controlled by AxioVision 4.8.2 with a ×20 lens. Images were captured every 3 min for 5 h with AxioVision 4.8.2.

Western blotting

Cells were collected and lysed with NP-40 lysis buffer (50 mM HEPES, pH 7.4, 200 mM KCl, 0.3% NP-40, 10% glycerol, 1 mM EGTA, 1 mM $MgCl_2$, 0.5 mM DTT, 0.5 μM microcystin, and 10 μg/ml concentrations of leupeptin, pepstatin, and chymostatin) on ice for 10 min and debris was removed by centrifugation. Protein concentrations in total cell lysates were measured using a Bradford protein assay kit before boiling in Laemmli buffer. Equal volumes of protein samples were loaded, separated by a 12% SDS-PAGE gel, and transferred to a PVDF membranes. The membranes were incubated overnight at 4°C with the primary antibodies, followed by incubation with the appropriate secondary antibodies. HRP-conjugated anti-mouse IgG or anti-rabbit IgG were used as secondary antibodies. Protein bands were detected using chemiluminescence blotting substrate (Roche, Switzerland) and X-ray film.

Purification of the DDA3 complex

HeLa S3 cell line stably expressing the GFP- and S-tagged DDA3 was established. The cells were synchronized at G1/S boundary by a single thymidine arrest and harvested at 8 h after release to purify mitotic complex. Tagged DDA3 complex was purified through two affinity steps (Cheeseman et al., 2004). The GFP-S-DDA3 fusion proteins were isolated using anti-GFP antibodies through immunoprecipitation with Protein A resin. TEV protease was treated to immunopresipitated proteins for overnight at 4°C. The cleaved protein was pulled-down with S protein beads and eluted using elution buffer (50 mM Tris [pH 8.5], 8 M urea) for analysis of interacting proteins using Mass spectrometry.

Cell synchronization

To arrest at G1/S boundary with a double thymidine block, cells were treated with 2 mM thymidine for 18 h, released into fresh medium for 8 h, and then incubated with 2 mM thymidine for 18 h (Fang et al., 1998). For synchronization at mitosis with thymidine-nocodazole block, cells were treated with 2 mM thymidine for 18 h, washed with PBS, cultured in fresh medium for 6 h, and then incubated with medium containing 100 ng/ml nocodazole for 12 h. After releasing into fresh medium, the cells were harvested at serial time points to analyze the level of proteins.

RNA isolation and real-time reverse transcription quantitative polymerase chain reaction (RT-qPCR)

Based on the genome sequence, qPCR primers were designed using the Primer-BLAST software at the National Center for Biotechnology Information. The primer sequences for GAPDH are 5′-GCC TGA GAA ACG GCT ACC A-3′ (forward) and 5′-GTC GGG AGT GGG TAA TTT GC-3′ (reverse) (NM_022551.3); CBL are 5′-GGA AGC ACG TTC AGT CTG CTG GA-3′ (forward) and 5′-GTA GAG GCC TGG AAG AGG GA-3′ (reverse) (NM_005188.4); DDA3 are 5′-TCT CCG GGC TAC ATC TGG AA-3′ (forward) and 5′-TTG CTG GTA GAA GGC TGT GG-3′ (reverse) (NM_032636.7); PLK4 are 5′-TAGG TAC TAG TTC ACC TAA GG-3′ (forward) and 5′-CAT AGA GGG ATT AAG GAT TG-3′ (reverse) (NM_014264.5); STIL are 5′-TAA TTT CAC CAA ACA ACA TG-3′ (forward) and 5′-TTC ATG GTC ATT CTT AGA AG-3′ (reverse) (NM_001048166.1).

Total RNA was isolated from HeLa cells using TRIzol reagent (15596026) (Invitrogen/Thermo Fisher Scientific) according to the manufacturer's protocol, and cDNAs were synthesized from 1 μg RNAs using the cDNA reverse transcription kit (4309155) (Invitrogen/Thermo Fisher Scientific). Real-time qPCR was carried out using the iScript cDNA Synthesis Kit (1708890) (Bio-Rad Laboratories). Cycling conditions were as described by manufacturer recommend. cDNA synthesis was performed using 1 μg of total RNA in 20 μl with random primers and iScript cDNA Synthesis Kit in a final volume of 10 μl. The relative mRNA expression of target genes in each RNA sample was calculated as copy numbers per GAPDH mRNA copy. Data analyses were performed using QuantStudio Design & Analysis software (Invitrogen/Thermo Fisher Scientific). The RNA concentration of each sample was determined by spectrophotometry at 260 nm; the integrity of each RNA sample was evaluated using the Gen5 (BioTek, USA). qPCR analyses were performed with SYBR-Green fluorescent dye using the QuantStudio3 system.

Statistical analysis

Data are represented as mean ± SEM. Statistical analyses

were performed with GraphPad Prism 8 software (GraphPad Software, USA); the Student's *t*-test was used to determine the significance of differences between experimental groups using. Error bars represent the SEM of three independent experiments. A *P* value less than 0.01 was considered statistically significant.

RESULTS AND DISCUSSION

c-Cbl acts as a mitotic regulator by interacting with DDA3 during mitosis

Because the expression levels of mitotic regulators during the cell cycle fluctuate according to the rates of synthesis and proteolysis, we purified the DDA3 complex from mitotic cells synchronized by thymidine-nocodazole treatment to determine the corresponding E3 ligase (Jang et al., 2008). Interestingly, c-Cbl was identified as a component of the DDA3 complex based on proteomic analysis by mass spectrometry (Fig. 1A). This association was verified in a transient transfection experiment involving coimmunoprecipitation of endogenous DDA3 with HA-c-Cbl but not empty vector (EV) (Fig. 1B). To investigate whether c-Cbl acts as a mitotic regulator, c-Cbl protein levels were examined throughout cell cycle. HeLa S3 cells were synchronized either at the G1/S boundary by a double thymidine treatment (Thy-Thy) or at prophase by thymidine-nocodazole treatment, and then placed into fresh media. The mitotic time points were determined by the levels of cyclin B. Strikingly, the level of c-Cbl increased during mitosis similar to the expression profile of cyclin B (Fig. 1C) and slightly decreased during mitotic exit (Fig. 1D), indicating that c-Cbl functions as a mitotic regulator via interaction with DDA3.

Although c-Cbl showed diffuse localization during mitosis, its depletion caused similar mitotic defects similar to those observed with DDA3 depletion, such as unaligned chromosomes at metaphase (Figs. 1E-1G). Time-lapse analysis of mitotic progression in HeLa cells stably expressing GFP-Histone H2B also indicated that c-Cbl-depletion induced chromosome alignment defects, leading to a lengthening of the duration from the initial formation of the metaphase plate to the onset of anaphase (Fig. 1H). Therefore, we concluded that c-Cbl regulates mitotic progression through interaction with DDA3 during mitosis.

c-Cbl acts as an E3 ligase that ubiquitinates DDA3 in mitosis

To investigate whether c-Cbl acts as an E3 ligase against DDA3, we examined the level of DDA3 and ubiquitinated DDA3 in c-Cbl-depleted cells. Although mRNA level of DDA3 was slightly decreased, the protein level of DDA3 was substantially increased by c-Cbl depletion (Figs. 2A and 2B). Consistent with this, the level of ubiquitinated DDA3 decreased in c-Cbl-depleted cells (Fig. 2A), suggesting that c-Cbl is a physiological E3 ligase for ubiquitin-mediated DDA3 degradation. To examine whether mitotic defects caused by c-Cbl-depletion resulted from the increment of DDA3 levels, we partially depleted DDA3 in c-Cbl-knockdown cells to maintain normal levels of DDA3 and found the rescue of unaligned chromosome (Figs. 2C and 2D).

Because c-Cbl depletion increased the levels of DDA3 in cell lysate, we next examined the recruitment of DDA3 recruitment to the mitotic spindle. As expected, the level of DDA3 on the spindle increased in c-Cbl-depleted cells (Fig. 2E). Because DDA3 facilitates minus-end MT depolymerization by recruiting the MT depolymerase, Kif2a (Jang et al., 2008; Kwon et al., 2016), we measured the level of Kif2a at the minus-end MT in c-Cbl-depleted cells and found an increase in the level of Kif2a near the spindle pole (Fig. 2F). Accordingly, depletion of c-Cbl resulted in a reduced amount of β-tubulin in mitotic spindle in metaphase cells (Fig. 2F) and overexpression of c-Cbl increased a level of β-tubulin (Fig. 2G). Because siCbl-1 and siCbl-2 target to the noncoding sequence of the endogenous c-Cbl gene, we ectopically expressed HA-c-Cbl in c-Cbl-depleted cells and found recovery of spindle formation (Fig. 2G). These data suggest that c-Cbl modulates the level of DDA3 on the mitotic spindle and the concomitant recruitment of Kif2a to regulate mitotic spindle assembly.

c-Cbl is involved in spindle dynamics and spindle MT attachment

As spindle formation is the dynamic process of polymerization and depolymerization of MTs in mitotic cells (Kline-Smith and Walczak, 2004), we directly measured the MT stability in c-Cbl knockdown cells. With 1 μg/ml nocodazole for 3 min, disruption of the mitotic spindle was faster in c-Cbl-depleted cells (Figs. 3A and 3B). To investigate MT polymerization in c-Cbl-depleted cells, spindle MTs were completely depolymerized with 1 μg/ml nocodazole treatment for 10 min and then placed into fresh media. Under facilitated MT depolymerization, the kinetics of MT repolymerization were substantially slower in c-Cbl-depleted cells (Figs. 3C and 3D). Given that spindle dynamics are essential for metaphase chromosome alignment and formation of the bipolar spindle (Kline-Smith and Walczak, 2004; Lee, 2014; Simunic and Toilc, 2016), we investigated the state of the spindle assembly checkpoint. Attachment of spindle MTs to the kinetochore (KT) and tension between sister KTs are monitored by Mad2 and BubR1, respectively (Musacchio and Salmon, 2007). Therefore, Mad2 and BurbR1 localized to KTs at prometaphase, but disappeared at metaphase in control cells (Figs. 3E and 3G). c-Cbl-depleted metaphase cells showed a fivefold increase in KT Mad2 signals for unaligned chromosomes out of the metaphase plate (Figs. 3E and 3F), indicating that c-Cbl-mediated spindle dynamics are essential for attachment of spindle MTs to KTs. Because a lack of MT attachment abolishes the tension across sister KTs, BubR1 remained on the KTs of unaligned chromosomes in c-Cbl-depleted metaphase cells (Figs. 3G and 3H). This indicates that c-Cbl regulates the spindle MT depolymerization, which, in turn, mediates the attachment of spindle MTs to KTs and the concomitant chromosome alignment at the metaphase plate.

c-Cbl is associated with the centrosome cycle and centriole duplication

Because the reduction in the protein level of c-Cbl by siRNA generated multipolar spindle (Fig. 4A), we analyzed centrosome and centriole integrity in c-Cbl-depleted cells. Surpris-

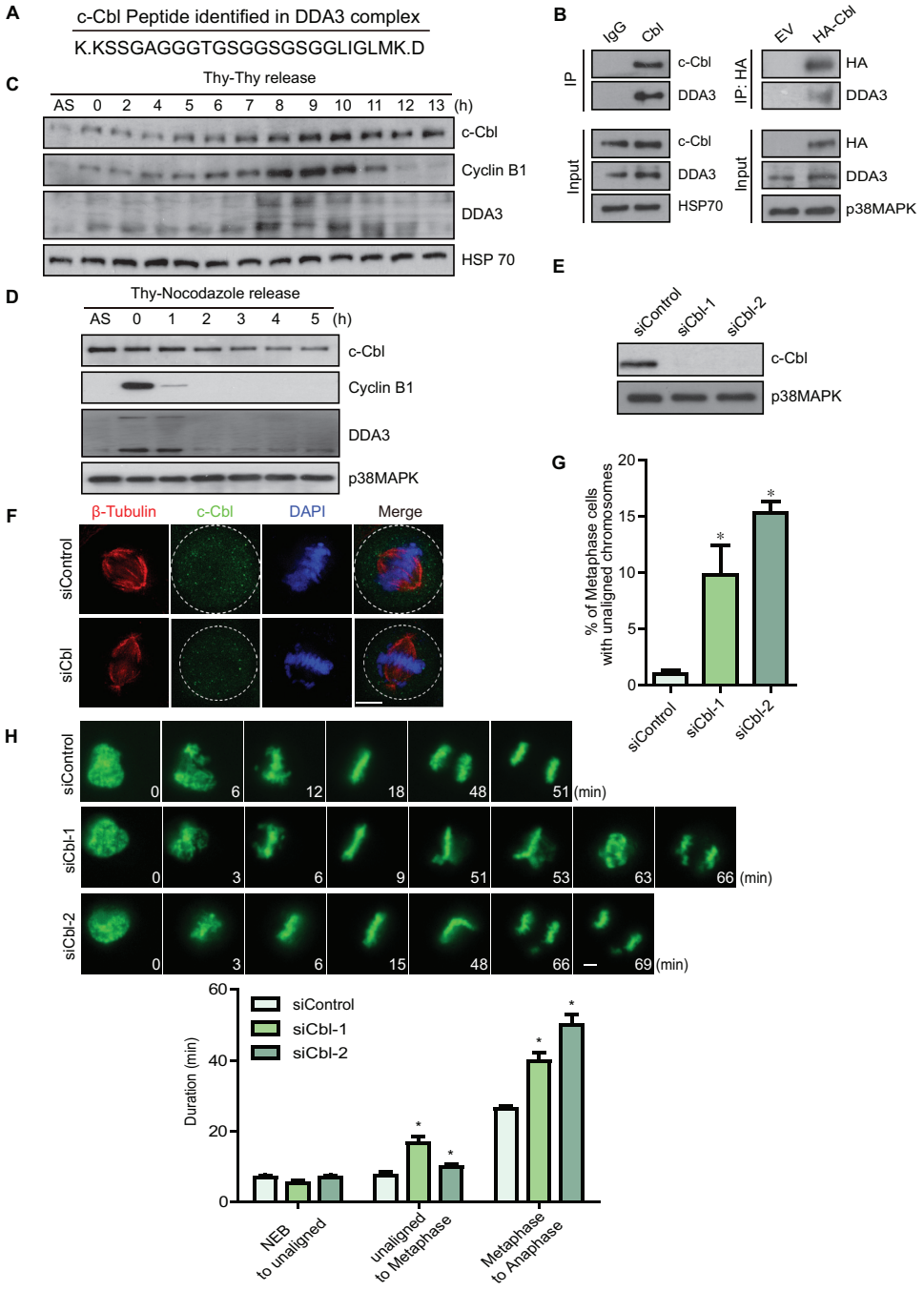

Fig. 1. c-Cbl interacts with DDA3 and acts as a mitotic regulator. (A) The DDA3 complex was purified from mitotic cells and analyzed by mass spectrometry. A peptide of c-Cbl was identified three times. (B) Twenty-eight hours after transfection of the EV or HA-c-Cbl plasmid, HeLa cells were harvested and subjected to immunoprecipitation and western blotting with the indicated antibodies. p38MAPK served as a loading control. EV, empty vector. (C and D) HeLa cells were synchronized by a double thymidine block (C) or thymidine-nocodazole block (D), placed into fresh media, and harvested at the indicated times. Cell lysates were analyzed by western blotting with the indicated antibodies. AS, unsynchronized cells. (E) HeLa cells were transfected with control (siControl) or c-Cbl-specific siRNAs (siCbl-A and siCbl-B). Seventy-two hours after siRNA transfection, the transfected cells were harvested and lysed to measure protein levels by western blotting with the indicated antibodies. (F and G) Seventy-two hours after siRNA transfection, HeLa cells were fixed with MeOH and stained with antibodies as indicated. Images are maximum projections from Z-stacks of representative cells stained for c-Cbl (green), β-tubulin (red), and DNA (blue). The number of metaphase cells with unaligned chromosomes was quantified and plotted (G) (n = 300 metaphase cells from three independent experiments). (H) Seventy-two hours after siRNA transfection, HeLa cells expressing GFP-Histone H2B cells were imaged for GFP fluorescence by time lapse. Images were captured every 3 min to monitor mitotic progression. NEB, nuclear envelop breakdown. Unaligned, the initial formation of the metaphase plate. Data are represented as mean ± SEM. Scale bars = 5 μm. $*P < 0.01$.

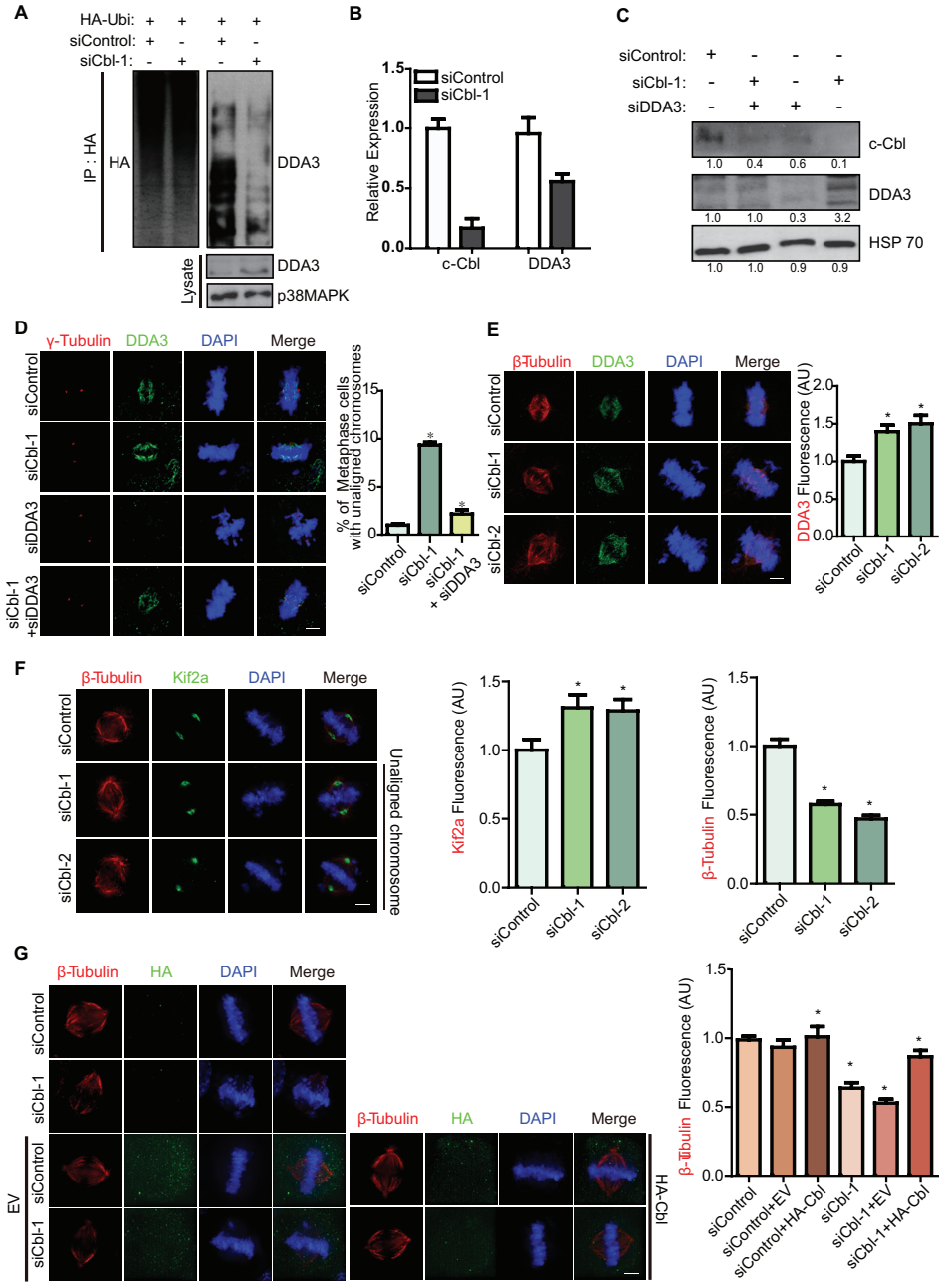

Fig. 2. c-Cbl modulates the levels of DDA3 and Kif2a at the mitotic spindle for spindle formation. (A) Forty-eight hours after siRNA transfection, HeLa cells were transfected with HA-Ubiquitin plasmid. Twenty-four hours after plasmid transfection, the cells were treated with 10 mM proteasome inhibitor, MG132, for 5 h and then harvested and subjected to immunoprecipitation and western blotting with the indicated antibodies. (B) Seventy-two hours after siRNA transfection, the cells were treated with nocodazole for 18 h. The mRNA levels of c-Cbl and DDA3 in mitotic cells were quantified by real-time RT-qPCR analysis (n = 3). (C and D) Seventy-two hours after siRNA transfection, HeLa cells were harvested to analyze protein levels with the indicated antibodies (C) or fixed with MeOH to analyze unaligned chromosomes in metaphase cells (D). Relative intensities of band were quantified by image processing software (C; Image Studio ver5.0). (E) Seventy-two hours after siRNA transfection, HeLa cells were fixed with MeOH and stained with antibodies as indicated. Images, which were acquired under a constant exposure time, are maximum projections from Z-stacks of representative cells. The intensity of DDA3 was quantified and plotted (n = 10 cells for each quantification). (F) HeLa cells were transfected with siRNA and prepared as in Figure 1E. For each quantification, the intensities of spindle and Kif2a were determined based on the immunofluorescence from 10 cells. (G) Forty-eight hours after siRNA transfection, HeLa cells were transfected with either the EV or HA-c-Cbl plasmid. The cells were fixed in MeOH and stained with β-tubulin antibody at 28 h after plasmid transfection. Images for β-tubulin were acquired under a constant exposure time and spindle intensity was quantified (n = 10 cells for each quantification). EV, empty vector; AU, arbitrary units. Data are represented as mean ± SEM. Scale bars = 5 μm. $*P < 0.01$.

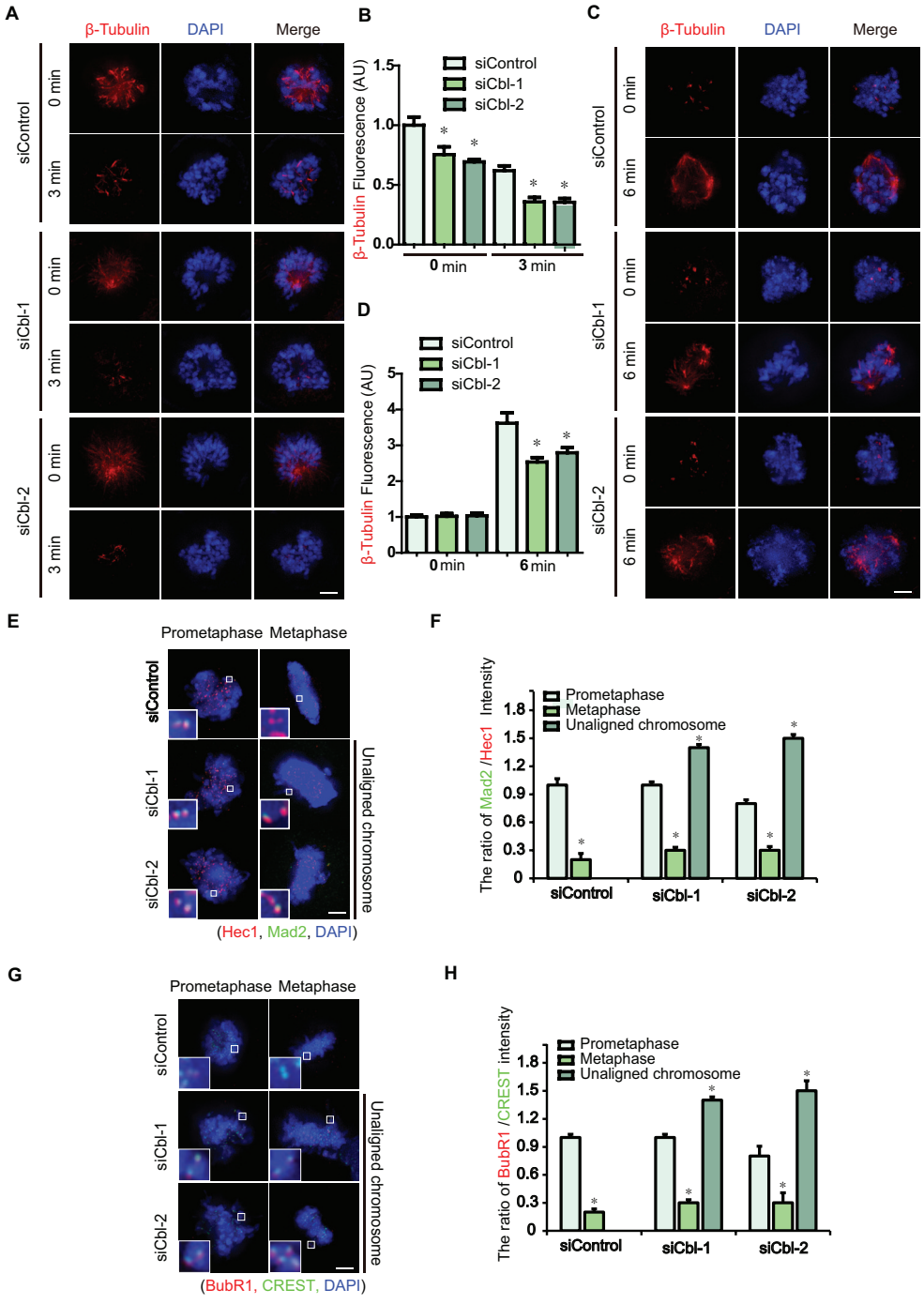

Fig. 3. c-Cbl controls spindle stability and spindle attachment to the kinetochore. (A and B) Seventy-two hours after siRNA transfection, HeLa cells were treated with 1 μg/ml nocodazole for 3 min, fixed in MeOH, and analyzed by immunofluorescence staining of β-tubulin. (C and D) After spindle disruption by treatment with 1 μg/ml nocodazole for 10 min, c-Cbl-depleted cells were placed in fresh media for 6 min and stained with β-tubulin antibody. The spindle intensity was quantified and plotted (n = 10 for each quantification). (E-H) Seventy-two hours after siRNA transfection, HeLa cells were stained with the indicated antibodies. The ratio of Mad2/Hec1 (F) or BubR1/CREST (H) ratios were quantified and plotted (n = 100 kinetochores from 10 cells for each quantification). AU, arbitrary units. Data are represented as mean ± SEM. Scale bars = 5 μm. $*P < 0.01$.

ingly, over-duplicated centrosomes achieved spindle bi-orientation by clustering multiple centrosomes and ultimately forming a pseudobipolar spindle in c-Cbl-depleted cells (Figs. 4A and 4B). Given that premature centriole disengagement is induced by inappropriate activation of separase in G2 or uncontrolled polo like kinase 1 (Plk1) activity in prophase (Tsou

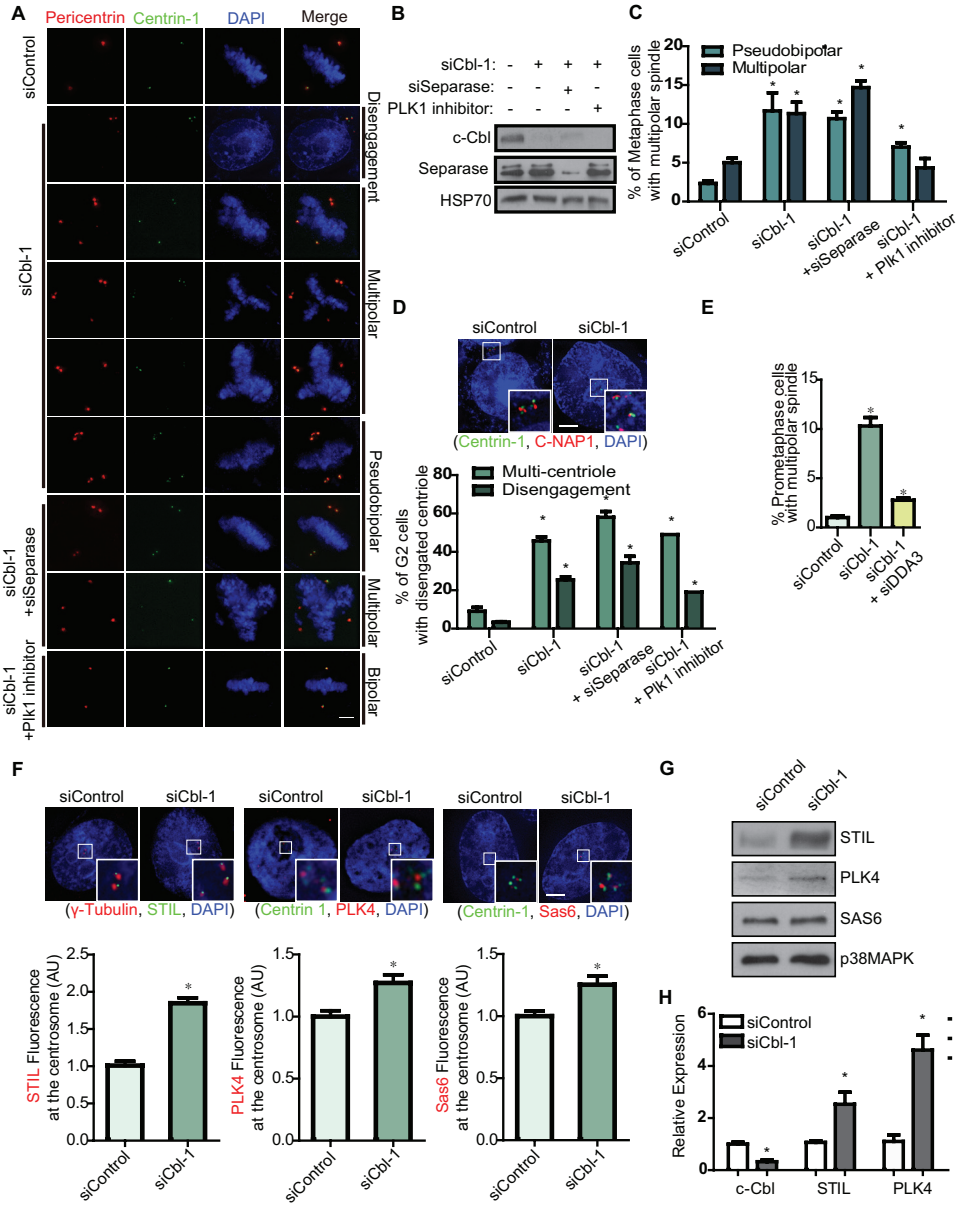

Fig. 4. c-Cbl is involved in centriole duplication. (A-C) HeLa cells were transfected with a siControl or siCbl for 72 h. The cells were cotreated with a separase siRNA (siSeperase) for 72 h or 100 nM BI 2536, as a Plk1 inhibitor, for 2 h. Images are maximum projections from Z-stacks of representative cells stained for Centrin-1 (green), β-tubulin (red), and DNA (blue). The level of proteins were analyzed by western blotting using the indicated antibodies (B). Metaphase cells with multipolar spindles or pseudobipolar spindles were quantified and plotted (C; n = 100 cells for each quantification). (D) Seventy-two hours after siRNA transfection, HeLa cells were fixed in MeOH and stained for Centrin-1 (green), C-NAP1 (red), and DNA (blue). G2 cells with multiple or disengaged centrioles were quantified and plotted (n = 100 cells for each quantification). (E) HeLa cells were transfected with siRNAs and prepared as in Figure 2D. Metaphase cells with multipolar spindles were quantified and plotted (n = 100 cells for each quantification). (F and G) HeLa cells were transfected with a siControl or siCbl. The cells were fixed in MeOH and stained with antibodies as indicated. The Sas6, STIL, and PLK4 intensities were quantified and plotted (n = 100 centrioles for each quantification). Alternatively, the cells were harvested at 72 h post-transfection and lysates were analyzed by western blotting using the indicated antibodies (G). (H) Seventy-two hours after siRNA transfection, the mRNA levels of c-Cbl and DDA3 in nocodazole-treated mitotic cells were quantified by RT-qPCR analysis (n = 3). AU, arbitrary units. Data are represented as mean ± SEM. Scale bars = 5 μm. $*P < 0.01$.

et al., 2009), we tested whether premature activation of separase or Plk1 is responsible for premature centriole disengagement in c-Cbl-depleted cells. While knockdown of separase did not rescue pseudobipolar and multipolar spindle in mitosis in c-Cbl-depleted cells, a partial rescue was observed with inhibition of Plk1 (Figs. 4B and 4C), suggesting that

depletion of Cbl induces hyper-activation of Plk1 and concomitant centrosome multipolarity. Furthermore, centrioles in duplicated centrosomes were amplified in c-Cbl-depleted cells (Fig. 4D). Among the duplicated centrosomes both in both pseudobipolar and multipolar spindles, we found that C-NAP1 foci at the distal ends of mother and daughter centrioles were separated by premature centriole disengagement (Fig. 4D). As Plk1 is also involved in centrosome separation (Meraldi and Nigg, 2002), treatment with a Plk1 inhibitor partially rescued premature disengagement of centriole in G2 in c-Cbl-depleted cells (Fig. 4D). Similar to unaligned chromosome, metaphase cells containing multipolar spindle rescued by partial depletion of DDA3 (Fig. 4E), suggesting that the increment of DDA3 causes multipolar spindle in c-Cbl-depleted cells. To investigate the reason for centriole amplification in c-Cbl-depleted cells, we measured the levels of the core proteins for centriole duplication, such as PLK4 and the centriolar assembly proteins STIL and Sas6 (Arquint and Nigg, 2016). Overexpression of any one of these three proteins results in centriole amplification. Strikingly, the levels of STIL and PLK4 increased substantially in c-Cbl-depleted cells (Figs. 4F and 4G). Consistent with this, mRNA levels of STIL and PLK4 substantially increased by c-Cbl-depletion (Fig. 4H), suggesting that c-Cbl mediates centriole duplication by modulating STIL and PLK4 expression through DDA3. However, the associated molecular mechanisms remain to be elucidated.

We identified c-Cbl, which modulates signaling pathway of RTK, as a new mitotic E3 ligase during mitosis. Although the levels of c-Cbl protein increased in mitosis (Fig. 1C), DDA3 levels increases during mitosis (Jang et al., 2008). Therefore, the E3 ligase activity of c-Cbl has to be regulated to maintain increased levels of DDA3 in mitosis. Because DDA3 is highly phosphorylated in mitosis (Jang et al., 2008), it is possible that c-Cbl might not be able to attach ubiquitin to phosphorylated DDA3. The redundancy between c-Cbl and ASP7 as mitotic E3 ligases against DDA3 remains to be elucidated.

In summary, we demonstrated that c-Cbl regulates spindle dynamics and chromosome alignment by acting as an E3 ligase that ubiquitinates DDA3 and modulating the amount of Kif2a at the minus-end of MTs. Furthermore, c-Cbl functions in the centrosome cycle and in centriole duplication by regulating Plk1 activity and the levels of STIL and PLK4 through DDA3. Our novel data clearly shows that c-Cbl is an essential mitotic regulator for the establishment of spindle bi-orientation, as well as for centriole duplication during mitosis.

Disclosure

The authors have no potential conflicts of interest to disclose.

ACKNOWLEDGMENTS

This study was supported in part by grants from the National Research Foundation of Korea (NRF-2015R1A2A-2A01005500 and NRF-2018R1D1A1B07050933).

ORCID

Dasom Gwon https://orcid.org/0000-0001-8863-9578
Jihee Hong https://orcid.org/0000-0002-1981-3760
Chang-Young Jang https://orcid.org/0000-0003-1177-3239

REFERENCES

Arquint, C. and Nigg, E.A. (2016). The PLK4-STIL-SAS-6 module at the core of centriole duplication. Biochem. Soc. Trans. *44*, 1253-1263.

Castro, A., Bernis, C., Vigneron, S., Labbe, J.C., and Lorca, T. (2005). The anaphase-promoting complex: a key factor in the regulation of cell cycle. Oncogene *24*, 314-325.

Cheeseman, I.M., Niessen, S., Anderson, S., Hyndman, F., Yates, J.R., 3rd, Oegema, K., and Desai, A. (2004). A conserved protein network controls assembly of the outer kinetochore and its ability to sustain tension. Genes Dev. *18*, 2255-2268.

Choi, Y.H., Han, Y., Lee, S.H., Jin, Y.H., Bahn, M., Hur, K.C., Yeo, C.Y., and Lee, K.Y. (2015). Cbl-b and c-Cbl negatively regulate osteoblast differentiation by enhancing ubiquitination and degradation of Osterix. Bone *75*, 201-209.

Dulic, V., Lees, E., and Reed, S.I. (1992). Association of human cyclin E with a periodic G1-S phase protein kinase. Science *257*, 1958-1961.

Fang, G., Yu, H., and Kirschner, M.W. (1998). The checkpoint protein MAD2 and the mitotic regulator CDC20 form a ternary complex with the anaphase-promoting complex to control anaphase initiation. Genes Dev. *12*, 1871-1883.

Grovdal, L.M., Stang, E., Sorkin, A., and Madshus, I.H. (2004). Direct interaction of Cbl with pTyr 1045 of the EGF receptor (EGFR) is required to sort the EGFR to lysosomes for degradation. Exp. Cell Res. *300*, 388-395.

Huang, B., Pei, H.Z., Chang, H.W., and Baek, S.H. (2018). The E3 ubiquitin ligase Trim13 regulates Nur77 stability via casein kinase 2α. Sci. Rep. *8*, 13895.

Hunter, S., Burton, E.A., Wu, S.C., and Anderson, S.M. (1999). Fyn associates with Cbl and phosphorylates tyrosine 731 in Cbl, a binding site for phosphatidylinositol 3-kinase. J. Biol. Chem. *274*, 2097-2106.

Jang, C.Y., Wong, J., Coppinger, J.A., Seki, A., Yates, J.R., 3rd, and Fang, G.W. (2008). DDA3 recruits microtubule depolymerase Kif2a to spindle poles and controls spindle dynamics and mitotic chromosome movement. J. Cell Biol. *181*, 255-267.

Jiang, X., Huang, F., Marusyk, A., and Sorkin, A. (2003). Grb2 regulates internalization of EGF receptors through clathrin-coated pits. Mol. Biol. Cell *14*, 858-870.

Jin, J., Cardozo, T., Lovering, R.C., Elledge, S.J., Pagano, M., and Harper, J.W. (2004). Systematic analysis and nomenclature of mammalian F-box proteins. Genes Dev. *18*, 2573-2580.

Kline-Smith, S.L. and Walczak, C.E. (2004). Mitotic spindle assembly and chromosome segregation: refocusing on microtubule dynamics. Mol. Cell *15*, 317-327.

Kwon, H.J., Park, J.E., Song, H., and Jang, C.Y. (2016). DDA3 and Mdp3 modulate Kif2a recruitment onto the mitotic spindle to control minus-end spindle dynamics. J. Cell Sci. *129*, 2719-2725.

Lee, H. (2014). How chromosome mis-segregation leads to cancer: lessons from BubR1 mouse models. Mol. Cells *37*, 713-718.

Meisner, H., Conway, B.R., Hartley, D., and Czech, M.P. (1995). Interactions of Cbl with Grb2 and phosphatidylinositol 3'-kinase in activated Jurkat cells. Mol. Cell Biol. *15*, 3571-3578.

Meraldi, P. and Nigg, E.A. (2002). The centrosome cycle. FEBS Lett. *521*, 9-13.

Musacchio, A. and Salmon, E.D. (2007). The spindle-assembly checkpoint in space and time. Nat. Rev. Mol. Cell Biol. *8*, 379-393.

Nakayama, K.I. and Nakayama, K. (2006). Ubiquitin ligases: cell-cycle control and cancer. Nat. Rev. Cancer *6*, 369-381.

Schmidt, M.H.H. and Dikic, I. (2005). The Cbl interactome and its functions. Nat. Rev. Mol. Cell Biol. *6*, 907-918.

Shrestha, N., Shrestha, H., Ryu, T., Kim, H., Simkhada, S., Cho, Y.C., Park, S.Y.,

Cho, S., Lee, K.Y., Lee, J.H., et al. (2018). δ-Catenin increases the stability of EGFR by decreasing c-Cbl interaction and enhances EGFR/Erk1/2 signaling in prostate cancer. Mol. Cells *41*, 320-330.

Simunic, J. and Toilc, I.M. (2016). Mitotic spindle assembly: building the bridge between sister K-fibers. Trends Biochem. Sci. *41*, 824-833.

Skaar, J.R. and Pagano, M. (2009). Control of cell growth by the SCF and APC/C ubiquitin ligases. Curr. Opin. Cell Biol. *21*, 816-824.

Tsou, M.F., Wang, W.J., George, K.A., Uryu, K., Stearns, T., and Jallepalli, P.V. (2009). Polo kinase and separase regulate the mitotic licensing of centriole duplication in human cells. Dev. Cell *17*, 344-354.

Uematsu, K., Okumura, F., Tonogai, S., Joo-Okumura, A., Alemayehu, D.H., Nishikimi, A., Fukui, Y., Nakatsukasa, K., and Kamura, T. (2016). ASB7 regulates spindle dynamics and genome integrity by targeting DDA3 for proteasomal degradation. J. Cell Biol. *215*, 95-106.

Wong, J. and Fang, G.W. (2006). HURP controls spindle dynamics to promote proper interkinetochore tension and efficient kinetochore capture. J. Cell Biol. *173*, 879-891.